Sensors & Actuators: B. Chemical 290 (2019) 73–78

Contents lists available at ScienceDirect

Sensors and Actuators B: Chemical

journal homepage: www.elsevier.com/locate/snb

Handheld, low-cost electronic device for rapid, real-time fluorescence-based detection of Hg^{2+}, using aptamer-templated ZnO quantum dots

S.C.G. Kiruba Daniel, Archiev Kumar, K. Sivasakthi, Chetan Singh Thakur*

NeuRonICS Lab, Department of Electronic Systems Engineering, Indian Institute of Science, Bengaluru, 560012, India

ARTICLE INFO

Keywords:
Mercury
Aptamer
ZnO
Quantum dot
Device

ABSTRACT

Mercury is one of the most acute toxic heavy metals at trace levels and its detection at parts per billion (ppb) scale in a low-cost, simple way remains challenging. Here, we report a novel "Turn-On" fluorescence sensor based on aptamer-templated ZnO quantum dots (QDs), which was further developed into an electronic detection device and utilized for the rapid detection of mercury ions (Hg^{2+}). Binding of Hg^{2+} with the aptamer leads to the formation of a duplex, T-Hg^{2+}-T, and this acts as a template for the formation of ZnO QDs. With an increase in the concentration of Hg^{2+}, we observed an increase in duplex formation, leading to enhancement in the fluorescence. The limit of detection of the device is 0.1 ppb (0.5 nM), and experimental analysis has a linear range of detection between 0.1 and 10,000 ppb. Electron microscopy studies ascertained the crystalline nature of the aptamer-templated ZnO QDs in the presence of Hg^{2+}. Finally, the sensing was implemented as a simple working electronic detection device prototype. A photodiode coupled with an LED source was connected to an Arduino Nanoboard for the development of the device. To the best of our knowledge, this is the first study to report an enhancement in the fluorescence of the aptamer-templated ZnO QDs with an increase in the concentration of Hg^{2+}. Moreover, this is the first report of an analyte addition during the synthesis of QDs, leading to fluorescence-based sensing of the added analyte. Thus, a novel fluorescence sensor based on aptamer-templated ZnO QDs has been demonstrated with high sensitivity and selectivity, resulting in a simple electronic detection device.

1. Introduction

Heavy metals are major water pollutants that contribute to some of the most profound lethal and fatal effects [1]. Among heavy metals, mercury poisoning or pollution leads to large-scale environmental and health impact, even at trace level concentrations [2,3]. The presence of Hg^{2+}, even at low levels, has been linked to autism, ailments in vital organs, defects in the immune system, and even death [1,4,5]. Detection of mercury at parts per billion (ppb) levels is very important for devising plans to control its pollution. Common strategies used for the detection of mercury and other heavy metal ions include Raman spectroscopy [6,7], atomic absorption spectroscopy (AAS) [8], mass spectroscopy (MS) [9], inductively coupled plasma mass spectroscopy (ICP-MS) [10], anodic stripping voltammetry (ASV) [11], high performance liquid chromatography (HPLC), liquid chromatography mass spectrometry (LC–MS), and infrared spectroscopy [12]. Most of these techniques are time-consuming and involve sophisticated instruments that need high maintenance and skilled manpower for their operation and interpretation of results. The currently available instruments are either expensive or bulky or both, which hinders their use as portable and affordable detection devices. Thus, there is a need to develop a simple, low-cost, handheld device for the detection of mercury on field [12].

Fluorescence-based sensing of Hg^{2+} has been majorly carried out by Hg^{2+} induced aggregation of fluorescent nanomaterials and FRET (fluorescence resonance energy transfer). Hg^{2+} induced aggregation of fluorescent nanomaterials leading to quenching of fluorescence and subsequent detection has been reported [13]. FRET based Hg^{2+} detection has also been reported widely. These include FRET between two fluorescent dyes [14], FRET between nanomaterial with dye [15], exogenous dye, and cleaved DNA with dye [16]. Conventionally, organic dyes were used for fluorescent sensing, but they are vulnerable to photobleaching. Inorganic quantum dots are quite resistant to photobleaching and possess broad absorbance spectra and narrow emission band, making them suitable candidates for fluorescence-based sensing. Several studies have focused on the use of fluorescent semiconductor nanomaterials for sensing [17–19].

The use of DNA, aptamers, and DNAzymes for sensing of heavy metals using multiple different mechanisms has been reported widely

* Corresponding author.
E-mail address: csthakur@iisc.ac.in (C.S. Thakur).

https://doi.org/10.1016/j.snb.2019.03.113
Received 16 November 2018; Received in revised form 9 March 2019; Accepted 25 March 2019
Available online 26 March 2019
0925-4005/

[12,17,20]. An aptamer is a short, single-stranded DNA or RNA sequence having high binding affinity towards an element, pesticide, explosive, pathogen, protein, or small molecule, and can be identified by the process of systematic evolution of ligands by exponential enrichment (SELEX). Aptamers are easy to synthesize, low cost, and are stable at ambient conditions [21]. Aptamer-functionalized quantum dots (QDs) have been utilized for the detection of different targets, including Hg^{2+} [22–24]. Even though DNA-templated QDs were reported for different applications [25,26], to our knowledge no work has been reported for analyte sensing using aptamer-templated QDs. Fluorescence quenching-based sensing has been recently reported for the sensing of Hg^{2+}, but the method has its own disadvantage that in real samples, quenching may happen due to various factors other than the presence of analyte [22,27]. Hence, "Turn-On" fluorescent sensors are better than fluorescence quenching-based sensors. However, aptamer-based or functional nucleic acid-based "Turn-On" fluorescent sensors have certain disadvantages, such as high cost of fluorescent probes or complicated modification of aptamers. The cost of ZnO-based QDs was reported to be less than that of cadmium or other semiconductor materials and fluorescent probes for bio/nanosensor applications. ZnO has unique electrical and optical properties, such as wide band gap at room temperature, which results in significant quantum confinement [28]. ZnO-based nanomaterials have numerous environmental advantages, such as lesser corrosion, low toxicity, more recyclability, and easier disposal, and are thus ideal candidates for sensing applications [29]. Previously, we have reported interference in the synthesis of silver nanoparticles, leading to absorbance-based sensing of analyte, wherein the reducing agent displayed affinity towards the analyte [30,31]. In the present study, we found that the addition of Hg^{2+} to the template aptamer, followed by the precursor and reducing agent, led to an increase in the formation of DNA duplexes, thereby resulting in an increase in the formation of the quantum dots and, hence, an enhancement in the fluorescence (Fig. 1A).

2. Materials and methods

Aptamers (10-base aptamer with the sequence TTTTTTTTTT) were synthesized and HPLC purified by Eurofin Genomics (Bengaluru, Karnataka, India). All chemicals were of analytical grade and were used as such at appropriate concentrations. Milli-Q water (18.2 ohms) was used for all reactions. Zinc acetate (0.33 g in 15 ml) and potassium hydroxide (2.8 g in 50 ml) were used as the precursor and reducing agent, respectively. Milli Q water was spiked with Hg^{2+} to obtain the respective concentrations of 0.1, 1, 10, 100, 1000 and 10,000 ppb (0.5 nM, 5 nM, 50 nM, 500 nM, 5000 nM and 50,000 nM respectively). For all the device experiments, we have used Hg^{2+} spiked in tap water taken from our institution. This water has a TDS (Total Dissolved Solids) value of 182 ppm. Initial sensing reactions were carried out in black UV transparent 96-well plates, followed by absorbance and fluorescence measurements using TECAN Infinite plate reader. X-ray photoelectron spectroscopy (XPS) and transmission electron microscopy (TEM) were carried out at the Centre for Nano Science and Engineering (CeNSE), Indian Institute of Science. For XPS analysis, freshly prepared sample was drop-casted on a silica wafer. Similarly, freshly prepared sample was drop-casted on carbon-coated copper grid for TEM analysis and imaged using a Titan Thermis TEM, at an accelerating voltage of 300 kV.

3. Results and discussion

In the present study, sensing has been carried out by analyte binding to the template aptamer and QD synthesis, rather than via the conventional route of synthesis followed by functionalization and sensing. A poly-T sequence (10bp) was used for the templated synthesis of ZnO QDs in the presence of Hg^{2+}. Further, Hg^{2+} was added to the template followed by the precursor and reducing agent. For control, water was added instead of Hg^{2+}. At a volume ratio of 50:30:18:20 (template:analyte–Hg^{2+}: precursor: reducing agent), the poly-T aptamer(1 μM) folds into a hairpin-like structure, leading to the templated synthesis of fluorescent ZnO QDs. Hg^{2+} has high affinity towards the

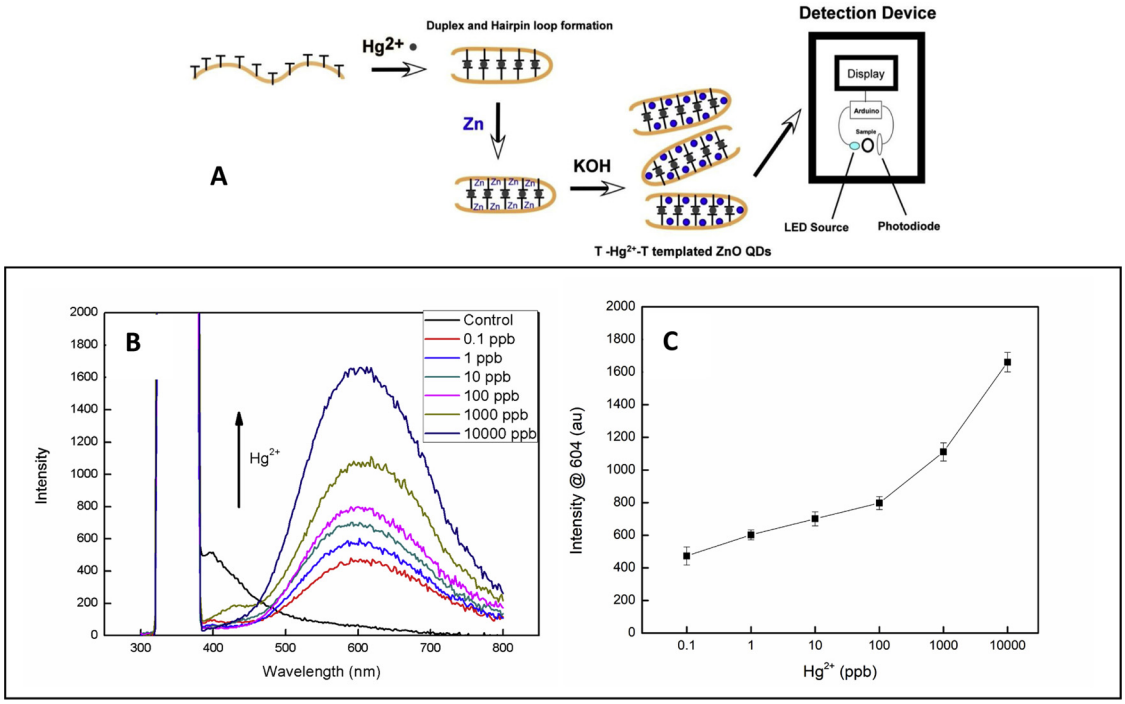

Fig. 1. Sensing mechanism is represented by a schematic representation and sensing emission peaks were presented. A) Schematic representation of the novel sensing mechanism utilized in the detection of Hg^{2+}, B) Fluorescence sensing graph exhibiting the gradual increase in the emission peak with increase in the concentration of Hg^{2+}during the synthesis of aptamer-templated ZnO QDs and C) Logarithmic data plot of the sensing graph with added error bar.

poly-T aptamer, and results in the formation of T–Hg^{2+}–T via strong covalent bonding of N3–Hg^{2+}–N3 [32]. Mismatch pairing in the T–Hg^{2+}–T duplex is very stable compared to the pairing in the Watson–Crick A—T bond and has been reported to have exhibited molecular ion peaks [33]. The T–Hg^{2+}–T duplex results in hairpin loop formation and has been utilized routinely for sensing of Hg^{2+} [12,34]. However, none of the previous methods reported the usage of the T–Hg^{2+}–T duplex for direct, simple QD fluorescence enhancement-based detection. The ratio of the reducing agent to the precursor and template was established after exhaustive trials with different molar concentrations of the reducing agent and precursor. With increase in the concentration of Hg^{2+}, there would be an increase in the formation of T–Hg^{2+}–T hairpin loops, leading to increase in the formation of ZnO QDs. Thus, as the ppb level of Hg^{2+} increases, there is an enhancement in the emission peak at 600 nm (Fig. 1B), which corresponds to the ZnO QD fluorescence with an excitation at 365 nm. The sensing has been done in triplicates and a data plot with error bar has been included in (Fig. 1C). Similarly, there is an enhancement in the absorbance of the ZnO QDs (Fig. S1) with increasing concentration of Hg^{2+}, which may be due to the increased formation of ZnO QDs. In the absence of Hg^{2+}, there is no duplex formation and, hence, no formation of ZnO QDs. Furthermore, the fluorescence intensity of ZnO QDs formed in the presence of 10 and 100 ppb Hg^{2+} which exhibits an initial increase and then decrease in emission with respect to time (Fig. S2).

The limit of detection (LOD) for Hg^{2+} was found to be 0.1 ppb (equivalent to 0.5 nM).This is well below the maximum permissible limit of 2 ppb Hg^{2+} in drinking water, as per the guidelines of the United States Environmental Protection Agency (USEPA) and World Health Organization (WHO) [35]. Elemental mapping of the ZnO QDs synthesized in the presence of Hg^{2+}, exhibited the presence of Hg^{2+} with ZnO QDs (Fig. 2 A, B, C, D, Fig. S3). In addition, high-resolution TEM (HRTEM) analysis showed a fringe pattern of the QDs, which revealed the crystalline nature and d-space value of 0.26 nm corresponding to ZnO (Fig. 2G) [18]. Analysis using ImageJ software showed that majority of the ZnO QDs formed were of size ~3 nm, as per the particle size histogram (Fig. 2H). However, few QDs of size ~6 nm were also found to have been formed, which may be due to various other factors such as aggregation or continuous growth of QDs on the aptamer duplex. Energy dispersive X-ray spectroscopy (EDX) confirms the presence of Zn, O and Hg^{2+} (Fig. S4).

In previous reports, nanoparticles or QDs were synthesized first, followed by functionalization with aptamers or antibodies or DNAzymes, and then exposure to analyte, leading to sensing. On the contrary, in this study, the analyte is added during the synthesis of QDs, leading to fluorescence-based sensing. This is the first report of an analyte addition leading to sensing by interfering in the synthesis of QDs. Previously, the addition of arsenic (at ppb levels) to synthesized ZnO QDs led to fluorescence quenching-based sensing in which the synthesis time of ZnO QDs is more than 12 h, and this was followed by sensing [18]. In addition, formation of ZnO QDs in the presence of Hg^{2+} has been confirmed in XPS analysis by the presence of Zn 2p peaks (Fig. 3A) which are otherwise absent in the absence of Hg^{2+} (Fig. 3E). In the present study, synthesis and sensing take place simultaneously, and the time for both is less than twenty minutes. Hence, the overall time taken for complete synthesis/sensing process is considerably less when compared to previously reported methods (Table 1). In the present study, synthesis and sensing occurs at ambient conditions without the requirement of specific temperature or pressure whereas in other reported fluorescent sensing methods require lengthy synthesis followed by conjugation processes.

Previous studies have shown that the major interfering agents during sensing of Hg^{2+} as Pb^{2+}, Cd^{2+}, Fe^{2+}, Cu^{2+}, Ni^{2+}, and Ag. These were used to ascertain the selectivity of the current fluorescence sensor, and not much significant fluorescence enhancement was observed in the presence of these ions (Fig. 4). Our method for the detection of Hg^{2+} based on aptamer-templated ZnO QDs requires considerably lower synthesis and sensing time and has a relatively better LOD (Table 1).

The first prototype, as shown in Fig. 5A, was an Arduino-based breadboard device. This device features a UV LED that emits UV light (365 nm), which after passing through the analyte solution is intercepted by the sensor, namely TSL235r. The sensor is a photodiode combined with a current-to-frequency converter. The TSL235r generates a square wave as an output, whose frequency is directly proportional to the intensity of illumination on the sensor area. This wave is then input to the computational board (Arduino Nano), which senses the frequency, computes the corresponding light intensity (mathematical calculations written in the code), and displays the frequency on the

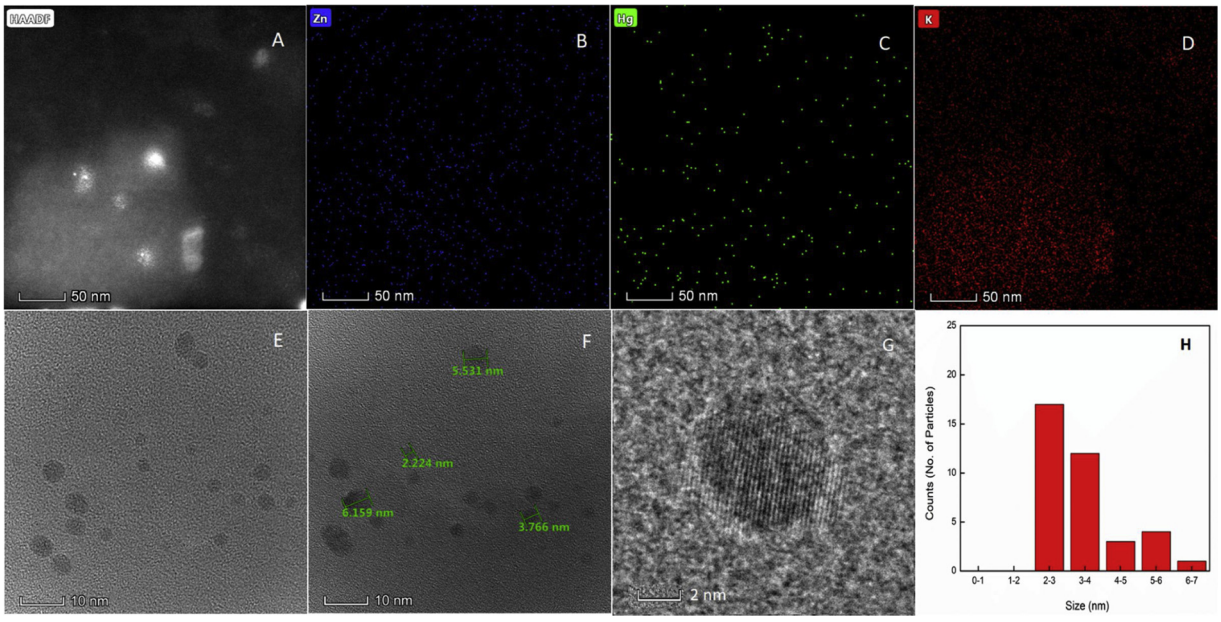

Fig. 2. High Angle Annular Dark Field (HAADF) STEM analysis of the sensing sample shows the presence of Hg with ZnO QDs at 50 nm scale by elemental mapping A) HAADF, B) zinc, C) mercury, D) potassium. Transmission electron microscopy images of aptamer-templated ZnO QDs with Hg^{2+} (100 ppb (500 nM)) at: E), F), 10 nm scale, G) High resolution TEM image exhibits fringe and H) particle size histogram.

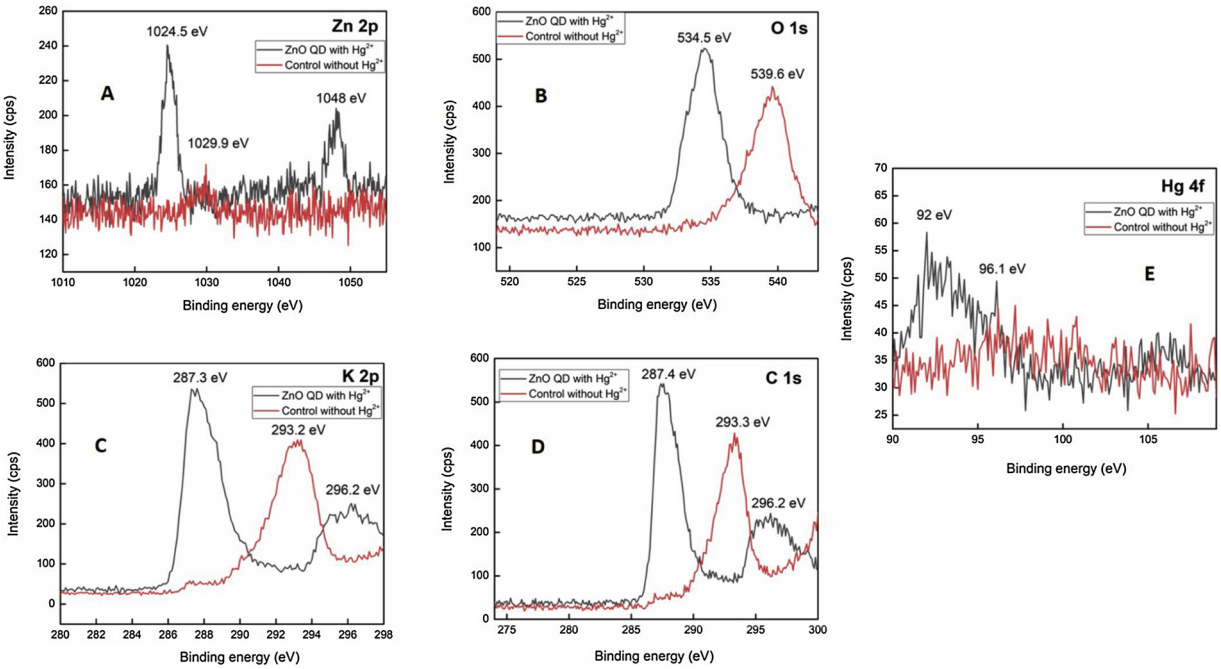

Fig. 3. XPS emission peaks of ZnO QDs were presented. A) Zn 2p, B) O 1s C) K 2p, D) C 1s and E) Hg 4f emission peaks of ZnO QDs formed in the presence of Hg^{2+} and control are presented. The presence of significant Zn 2p peak and its absence in control establishes the formation of ZnO QDs only in the presence of Hg^{2+}.

Table 1
Comparison of different sensing methods for the detection of Hg^{2+} based on their synthesis/sensing time and LOD.

Method	Material	Synthesis Time	Sensing Time	LOD	Reference
Colorimetry	Graphene Oxide Gold Nanohybrids	One week	15 min	300 nM	[36]
Fluorescence	Gold nanoparticles-conjugated aptamers	2 h	10 min	121 pM	[37]
Fluorescence	Oligonucleotide-functionalized Silver nanoparticles	1 h	1 hour	3 pM	[38]
Fluorescence	Organic Fluorescent Molecule	12 h	30 min	50 nM	[39]
Fluorescence	MPA-capped Mn-doped ZnSe/ ZnS Quantum Dots	6 h	30 seconds	0.1 nM	[22]
Colorimetry	Aptamer-coated gold nanoparticles	12 h	20 min	3 nM	[40]
Electrochemical Impedance Spectroscopy	DNA Gold Electrode films	5 days	Not mentioned	1 pM	[41]
Colorimetry	Photonic Hydrogel	12 h	30 min	10 nM	[42]
Fluorescence	Aptamer-templated ZnO QD	20 min		0.5 nM (0.1 ppb)	Current Method

OLED Display. The intensity of the light can be noted via the serial monitor, if required. This setup was used to test the sensing method proposed here and the accuracy was measured up to 0.1 ppb (0.5 nM). The frequency versus ppb concentration of Hg^{2+} has been plotted graphically (Fig. 5B), demonstrating the efficiency of the detection device. The block diagram of the device is shown in Fig. 5C. In addition, the fluorescence of the ZnO QDs can be observed under UV LED illumination, using a smart phone (Fig. S5). The initial breadboard prototype was modified and condensed into a 5 × 7 cm custom-made PCB, which resulted in a smaller footprint and greater scalability (Fig. 5D). A 3-D printed case was used to isolate the LED, TSL235 r, and the microtube, which prevents any ambient light interference or noise. There

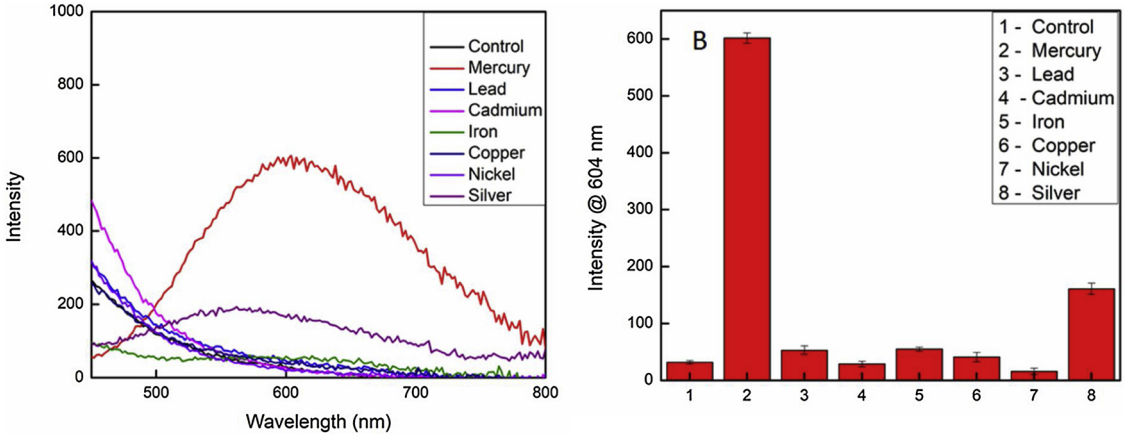

Fig. 4. Selectivity test shows the fluorescence peak of ZnO QDs in the presence of Hg^{2+}, compared to that in presence of six other heavy metal ions: lead, cadmium, iron, and copper. A) Selectivity test graph of wavelength versus fluorescence intensity. B) Selectivity bar diagram of fluorescence intensity at 604 nm.

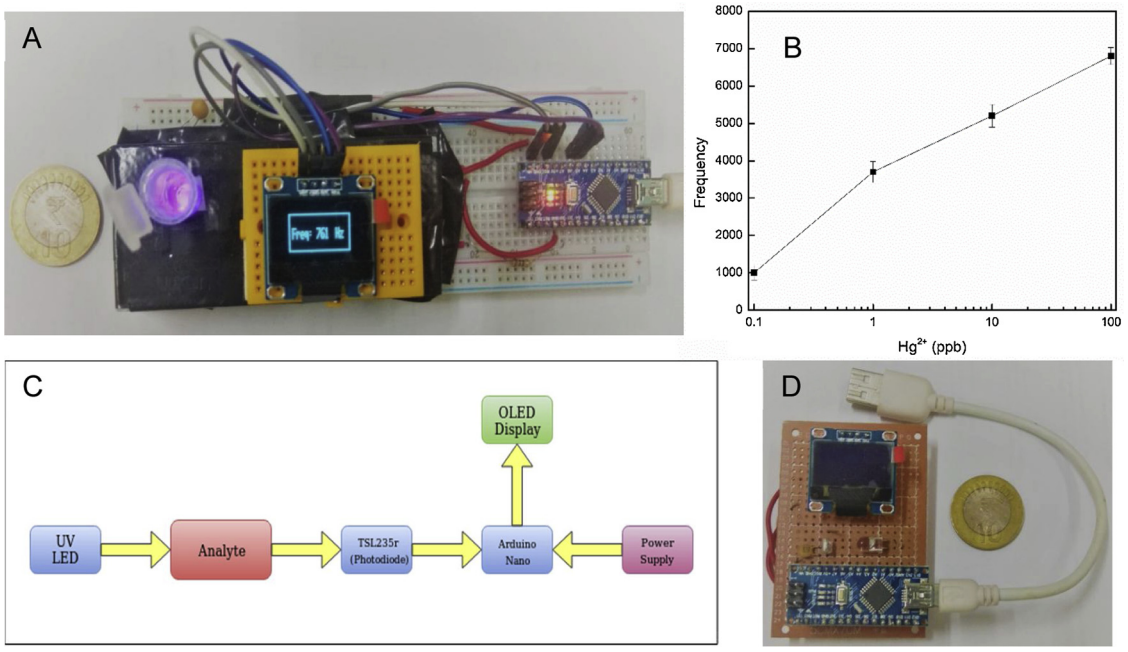

Fig. 5. Handheld device developed for the detection of Hg^{2+}, using aptamer-templated ZnO QDs. A) Breadboard-based detection prototype compared with a Rupee (INR) coin, B) Sensing graph (with error bar) exhibiting an increase in the frequency which is directly proportional to an increase in the fluorescence of ZnO QDs with increasing concentrations of Hg^{2+}, C) Block diagram of the components in the device, and D) Miniaturized prototype.

was a 12 mm gap between the LED and the sensor, which is where the microtube fits in. This arrangement not only cuts down the cost of the device, but also makes it highly portable and efficient.

4. Conclusions

A novel, highly sensitive and selective "Turn-On" fluorescence sensor utilizing aptamer-templated ZnO QDs has been demonstrated. For the first time, direct fluorescence enhancement of the ZnO QDs has been observed with increasing concentration of Hg^{2+}, which can be attributed to the formation of mismatch pair T–Hg^{2+}–T. T–Hg^{2+}–T pairing results in a hairpin loop-like structure, which enables the nucleation and growth of ZnO QDs. Thus, with an increase in the formation of T–Hg^{2+}–T, there is an increase in the formation ZnO QDs, resulting in enhanced fluorescence. The method has been successfully converted to a working, low-cost electronic device with an LED source and a photodiode. An LOD of 0.1 ppb (0.5 nM) of Hg^{2+} has been achieved using this device. TEM analysis confirmed the formation of ZnO QDs, with crystalline nature and an average size of 3 nm. In conventional sensors, synthesis followed by functionalization occurs before sensing. In contrast, in the present work, synthesis of ZnO QDs and sensing of Hg^{2+} is taking place simultaneously. Further commercialization of the novel sensor with the detection unit as a low-cost electronic device will enable detection of trace levels of mercury in resource-poor settings. Handheld device can be utilized in every household to detect any possible mercury contamination. For a commercially viable sensor device, it would be important that the development of a sensor is simple, which is highly achievable with the present work.

Acknowledgements

This work was financially supported by the DST Inspire Fellowship of Govt. of India DST_INSPIRE/DSTO-1776) and the Pratiksha Trust (PratikshaYI/2017-8512). Daniel would like to acknowledge the financial support received from SERB NPDF (PDF_2018_001929).

Appendix A. Supplementary data

Supplementary material related to this article can be found, in the online version, at doi:https://doi.org/10.1016/j.snb.2019.03.113.

References

[1] L. Magos, T. Clarkson, Overview of the clinical toxicity of mercury, Ann. Clin. Biochem. 43 (4) (2006) 257–268.
[2] H. Harris, I. Pickering, G. George, The chemical form of mercury in fish, Science 301 (5637) (2003) 1203.
[3] A.-T. Vo, M. Bank, J. Shine, S. Edwards, Temporal increase in organic mercury in an endangered pelagic seabird assessed by century-old museum specimens, Proc. Natl. Acad. Sci. 108 (18) (2011) 7466–7471.
[4] S. Bernard, A. Enayati, L. Redwood, H. Roger, T. Binstock, Autism: a novel form of mercury poisoning, Med. Hypotheses 56 (4) (2001) 462–471.
[5] C. Garza-Lombó, Y. Posadas, L. Quintanar, M. Gonsebatt, R. Franco, Neurotoxicity linked to dysfunctional metal ion homeostasis and xenobiotic metal exposure: redox signaling and oxidative stress, Antioxid. Redox Signal. 28 (18) (2018) 1669–1703.
[6] A. Kandjani, Y. Sabri, M. Mohammad-Taheri, V. Bansal, S. Bhargava, Detect, remove and reuse: a new paradigm in sensing and removal of Hg (II) from wastewater via SERS-active ZnO/Ag nanoarrays, Environ. Sci. Technol. 49 (3) (2015) 1578–1584.
[7] Z. Sun, J. Du, K. He, C. Jing, T-Hg^{2+}-T-based satellite structured surface enhanced Raman scattering sensor for Hg^{2+} detection, J. Raman Spectrosc. (2018).
[8] N. Bloom, W. Fitzgerald, Determination of volatile mercury species at the picogram level by low-temperature gas chromatography with cold-vapour atomic fluorescence detection, Anal. Chim. Acta 208 (C) (1988) 151–161.
[9] M. Wang, W. Feng, J. Shi, F. Zhang, B. Wang, M. Zhu, et al., Development of a mild mercaptoethanol extraction method for determination of mercury species in biological samples by HPLC–ICP-MS, Talanta 71 (5) (2007) 2034–2039.
[10] D. Karunasagar, J. Arunachalam, S. Gangadharan, Development of a' collect and punch' cold vapour inductively coupled plasma mass spectrometric method for the direct determination of mercury at nanograms per litre levels, J. Anal. At. Spectrom. 13 (7) (1998) 679–682.
[11] S.-H. Wu, Z.-Y. Zheng, J.-F. Zhang, Z.-W. Song, L. Fang, J.-J. Sun, Sub-ppt level detection of mercury(II) based on anodic stripping voltammetry with prestripping step at an in situ formed bismuth film modified glassy carbon electrode, Electroanalysis 27 (7) (2015) 1610–1615.
[12] Z. Khoshbin, M. Housaindokht, A. Verdian, M. Bozorgmehr, Simultaneous detection and determination of mercury (II) and lead (II) ions through the achievement of novel functional nucleic acid-based biosensors, Biosens. Bioelectron. 116 (2018) 130–147.
[13] Y. Ding, S. Wang, J. Li, L. Chen, Nanomaterial-based optical sensors for mercury ions, Trac Trends Anal. Chem. 82 (2016) 175–190.
[14] A. Ono, H. Togashi, Highly selective oligonucleotide-based sensor for mercury (II) in aqueous solutions, Angew. Chemie 116 (33) (2004) 4400–4402.

[15] D. Dinda, B.K. Shaw, S.K. Saha, Thymine functionalized graphene oxide for fluorescence “Turn-off-on” sensing of Hg2+ and I–in aqueous medium, ACS Appl. Mater. Interfaces 7 (27) (2015) 14743–14749.
[16] N. Xia, F. Feng, C. Liu, R. Li, W. Xiang, H. Shi, L. Gao, The detection of mercury ion using DNA as sensors based on fluorescence resonance energy transfer, Talanta (2018).
[17] W. Zhou, R. Saran, J. Liu, Metal sensing by DNA, Chem. Rev. 117 (12) (2017) 8272–8325.
[18] S. Pal, N. Akhtar, S. Ghosh, Determination of arsenic in water using fluorescent ZnO quantum dots, Anal. Methods 8 (2) (2016) 445–452.
[19] W. Chan, S. Nie, Quantum dot bioconjugates for ultrasensitive nonisotopic detection, Science 281 (5385) (1998) 2016–2018.
[20] J. Huang, X. Su, Z. Li, Metal ion detection using functional nucleic acids and nanomaterials, Biosens. Bioelectron. 96 (2017) 127–139.
[21] K. Srinivasan, K. Subramanian, K. Murugan, G. Benelli, K. Dinakaran, Fluorescence quenching of MoS2 nanosheets/DNA/silicon dot nanoassembly: effective and rapid detection of Hg2+ ions in aqueous solution, Environ. Sci. Pollut. Res. - Int. 25 (11) (2018) 10567–10576.
[22] J. Ke, X. Li, Q. Zhao, Y. Hou, J. Chen, Ultrasensitive quantum dot fluorescence quenching assay for selective detection of mercury ions in drinking water, Sci. Rep. 4 (2014) 5624.
[23] J. Choi, K. Chen, M. Strano, Aptamer-capped nanocrystal quantum dots: a new method for label-free protein detection, J. Am. Chem. Soc. 128 (49) (2006) 15584–15585.
[24] C. Zhang, X. Ji, Y. Zhang, G. Zhou, X. Ke, H. Wang, et al., One-pot synthesized aptamer-functionalized CdTe:Zn2+ quantum dots for tumor-targeted fluorescence imaging in vitro and in vivo, Anal. Chem. 85 (12) (2013) 5843–5849.
[25] W. Wei, X. He, N. Ma, DNA-templated assembly of a heterobivalent quantum dot nanoprobe for extra- and intracellular dual-targeting and imaging of live cancer cells, Angew. Chemie Int. Ed. 53 (22) (2014) 5573–5577.
[26] L. Zhang, S. Jean, S. Ahmed, P. Aldridge, X. Li, F. Fan, et al., Multifunctional quantum dot DNA hydrogels, Nat. Commun. 8 (1) (2017) 381.
[27] J. Li, H. Wang, Z. Guo, Y. Wang, H. Ma, X. Ren, et al., A “turn-off” fluorescent biosensor for the detection of mercury (II) based on graphite carbon nitride, Talanta 162 (2017) 46–51.
[28] J. Joo, S. Kwon, J. Yu, T. Hyeon, Synthesis of ZnO nanocrystals with cone, hexagonal cone, and rod shapes via non-hydrolytic ester elimination sol–gel reactions, Adv. Mater. 17 (15) (2005) 1873–1877.
[29] V. Coleman, C. Jagadish, Basic properties and applications of ZnO, in: V. Coleman, C. Jagadish (Eds.), Zinc Oxide Bulk, Thin Films and Nanostructures, Elsevier, 2006, pp. 1–20.
[30] S. Daniel, L. Nirupa Julius, S. Gorthi, Instantaneous detection of melamine by interference biosynthesis of silver nanoparticles, Sens. Actuators B Chem. 238 (2017) 641–650.
[31] S. Varun, S. Kiruba Daniel, S. Gorthi, Rapid sensing of melamine in milk by interference green synthesis of silver nanoparticles, Mater. Sci. Eng. C 74 (2017) 253–258.
[32] I. Onyido, A. Norris, E. Buncel, Biomolecule−Mercury Interactions: Modalities of DNA Base−Mercury Binding Mechanisms. Remediation Strategies, Chem. Rev. 104 (12) (2004) 5911–5930.
[33] Y. Miyake, H. Togashi, M. Tashiro, H. Yamaguchi, S. Oda, M. Kudo, et al., MercuryII-mediated formation of thymine−HgII−thymine base Pairs in DNA duplexes, J. Am. Chem. Soc. 128 (7) (2006) 2172–2173.
[34] G. Zhu, C.-y. Zhang, Functional nucleic acid-based sensors for heavy metal ion assays, Analyst 139 (24) (2014) 6326–6342.
[35] M. Update, Impact on fish advisories, EPA Fact Sheet (2001) EPA-823-F-01-011.
[36] X. Chen, N. Zhai, J. Snyder, Q. Chen, P. Liu, L. Jin, et al., Colorimetric detection of Hg 2+ and Pb 2+ based on peroxidase-like activity of graphene oxide–gold nanohybrids, Anal. Methods 7 (5) (2015) 1951–1957.
[37] C. Chung, J. Kim, J. Jung, B. Chung, Nuclease-resistant DNA aptamer on gold nanoparticles for the simultaneous detection of Pb2+ and Hg2+ in human serum, Biosens. Bioelectron. 41 (2013) 827–832.
[38] Z.-H. Wu, J.-H. Lin, W.-L. Tseng, Oligonucleotide-functionalized silver nanoparticle extraction and laser-induced fluorescence for ultrasensitive detection of mercury (II) ion, Biosens. Bioelectron. 34 (1) (2012) 185–190.
[39] S. Das, A. Sarkar, A. Rakshit, A. Datta, A sensitive water-soluble reversible optical probe for Hg2+ detection, Inorg. Chem. 57 (9) (2018) 5273–5281.
[40] L. Tan, Z. Chen, C. Zhang, X. Wei, T. Lou, Y. Zhao, Colorimetric detection of Hg2+ based on the growth of aptamer-coated AuNPs: the effect of prolonging aptamer strands, Small 13 (14) (2017) 1603370.
[41] L. Shi, G. Liang, X. Li, X. Liu, Impedimetric DNA sensor for detection of Hg 2+ and Pb 2+, Anal. Methods 4 (4) (2012) 1036–1040.
[42] B.-F. Ye, Y.-J. Zhao, Y. Cheng, T.-T. Li, Z.-Y. Xie, X.-W. Zhao, et al., Colorimetric photonic hydrogel aptasensor for the screening of heavy metal ions, Nanoscale 4 (19) (2012) 5998–6003.